Eur Radiol (2013) 23:597–606
DOI 10.1007/s00330-012-2656-2

COMPUTED TOMOGRAPHY

Image quality of ultra-low radiation exposure coronary CT angiography with an effective dose <0.1 mSv using high-pitch spiral acquisition and raw data-based iterative reconstruction

Annika Schuhbaeck · Stephan Achenbach · Christian Layritz · Jasmin Eisentopf · Franziska Hecker · Tobias Pflederer · Soeren Gauss · Johannes Rixe · Willi Kalender · Werner G. Daniel · Michael Lell · Dieter Ropers

Received: 11 June 2012 / Revised: 29 July 2012 / Accepted: 14 August 2012 / Published online: 16 September 2012

Abstract
Objectives We evaluated the potential of prospectively ECG-triggered high-pitch spiral acquisition with low tube voltage and current in combination with iterative reconstruction to achieve coronary CT angiography with sufficient image quality at an effective dose below 0.1 mSv.
Methods Contrast-enhanced coronary dual source CT angiography (2×128×0.6 mm, 80 kV, 50 mAs) in prospectively ECG-triggered high-pitch spiral acquisition mode was performed in 21 consecutive individuals (body weight <100 kg, heart rate ≤60/min). Images were reconstructed with raw data-based filtered back projection (FBP) and iterative reconstruction (IR). Image quality was assessed on a 4-point scale (1 = no artefacts, 4 = unevaluable).
Results Mean effective dose was 0.06±0.01 mSv. Image noise was significantly reduced in IR (128.9±46.6 vs. 158.2±44.7 HU). The mean image quality score was lower for IR (1.9±1.1 vs. 2.2±1.0, $P<0.0001$). Of 292 coronary segments, 55 in FBP and 40 in IR ($P=0.12$) were graded "unevaluable". In patients with a body weight ≤75 kg, both in FBP and in IR, the rates of fully evaluable segments were significantly higher in comparison to patients >75 kg.
Conclusions Coronary CT angiography with an estimated effective dose <0.1 mSv may provide sufficient image quality in selected patients through the combination of high-pitch spiral acquisition and raw data-based iterative reconstruction.
Key Points
- *Coronary CT angiography with an estimated effective dose <0.1 mSv is possible.*
- *Combination of high-pitch spiral acquisition with iterative reconstruction achieves sufficient image quality.*
- *Diagnostic accuracy remains to be assessed in future trials.*

Keywords Ultra low-dose coronary CT angiography · High-pitch spiral acquisition · Dual source CT · Iterative reconstruction · Image quality

A. Schuhbaeck (✉) · S. Achenbach · F. Hecker · J. Rixe
Department of Cardiology, University of Gießen,
Klinikstr. 33,
35392 Gießen, Germany
e-mail: annika.schuhbaeck@hotmail.de

C. Layritz · J. Eisentopf · T. Pflederer · S. Gauss · W. Kalender · W. G. Daniel · M. Lell · D. Ropers
Departments of Cardiology and Radiology,
University of Erlangen,
Erlangen, Germany

Introduction

Coronary computed tomography (CT) angiography permits visualisation of the coronary arteries and detection of coronary artery stenoses with high diagnostic accuracy [1–5]. Radiation exposure can be high and has been an area of critique [6, 7]. As a consequence, various techniques have been developed to reduce the radiation exposure associated with coronary CT angiography. Wider detector coverage and increased rotation speed of high-end CT systems have made the development of new data acquisition protocols possible, such as prospectively ECG-triggered axial acquisition [8, 9] or, very recently, prospectively ECG-triggered high-pitch spiral acquisition. These protocols are associated with

substantially lower dose than conventional spiral (also called "helical") acquisition. In some studies, effective dose values below 1.0 mSv have been reported [10, 11]. One potential disadvantage of the new data acquisition protocols as compared to conventional, retrospectively ECG-gated spiral or helical acquisition is loss of the ability to reconstruct data in various cardiac phases. Lowering tube voltage and tube current also leads to reduced exposure [6, 12]. However, both will result in increased image noise and may hence affect image quality [13–16]. Increased image noise may be offset by "iterative reconstruction" techniques. They can be used instead of traditional "filtered back projection" (FBP), which used to be the standard CT reconstruction algorithm because of the high reconstruction speed. As computational power has improved, raw data-based iterative reconstruction algorithms have been introduced by all vendors [17–21] and can now be performed fast enough for clinical applications. Several studies investigating the use of iterative reconstruction algorithms have demonstrated their potential to further reduce the radiation dose for the body [17], chest [22], abdominal [23] and cardiac imaging, including coronary CT angiography [18–21, 24, 25] without substantial impairment in image quality.

In the series of patients reported here, we evaluated the potential of a combination of these techniques to achieve coronary CT angiography with sufficient image quality at an effective dose below 0.1 mSv.

Materials and methods

Twenty-one consecutive patients with a body weight <100 kg and heart rate ≤60 beats per minute after premedication were included. All had been referred for coronary CT angiography to rule out coronary stenosis and gave informed consent to participate in the study.

Patients presenting with a heart rate >65 beats per minute (bpm) received 50 or 100 mg atenolol orally at least 30 min before the CT examination. If the heart rate remained >65 bpm in inspiration, up to 30 mg metoprolol was injected intravenously using repeated 5-mg doses before CT. Immediately before coronary CT angiography, all patients received 0.8 mg glycerol trinitrate sublingually.

Imaging was performed using second-generation Dual Source CT (Definition Flash, Siemens Healthcare, Forchheim, Germany, 280 ms rotation, 2×128×0.6 mm collimation) in deep inspiration. For all patients, tube voltage was set to 80 kV and tube current was 50 mAs.

A timing bolus protocol was used: 10 ml of contrast agent (Iomeprol, Imeron 350, Bracco Altana Pharma GmbH, Konstanz, Germany) was injected at a flow rate of 5 ml/s, followed by 50 ml of saline at the same flow rate. The time to peak enhancement in the ascending aorta was measured by obtaining a series of axial CT images acquired in 2-s increments, with the first image being acquired 15 s after the start of injection. For coronary CT angiography, 60 ml of contrast agent was injected, followed by a 60-ml flush (consisting of 80 % saline and 20 % contrast agent), both at the same flow rate of 6 ml/s. Image acquisition was initiated with a delay corresponding to the contrast agent transit time plus 4 s. Coronary CT angiography data sets were acquired using prospectively ECG-triggered high-pitch spiral acquisition, with the first image acquired at 55 % of the R-peak-to-R-peak interval [10].

CT image reconstruction

CT angiography images were reconstructed with traditionally filtered back projection (FBP) with 0.6-mm slice thickness and an increment of 0.3 mm using a medium smooth reconstruction kernel (Siemens "B26f"). The same raw data were transferred to an offline workstation, and images were reconstructed using a sinogram affirmed iterative reconstruction algorithm (SAFIRE, Siemens Healthcare, Forchheim, Germany) with the same slice thickness and increment. SAFIRE uses a noise modelling technique supported by the raw data. The local noise content in each image pixel is estimated by analysing the raw data contribution to this pixel and then removed from the image data set by the SAFIRE reconstruction algorithm. This can be done in several strength levels. Currently, up to five levels can be performed in the commercial version of the software [17, 20]. In our study, we used level 3 in all patients.

Image quality

Image quality was assessed by two independent observers in coronary CT angiography images reconstructed with FBP and SAFIRE. Observers read all data sets in random order and were blinded as to the image reconstruction method of each data set.

Image quality was evaluated using a 4-point scale: (1 = no artefacts, 2 = fully interpretable with mild artefacts, 3 = interpretable regarding the presence of stenoses in spite of moderate artefact, 4 = unevaluable) on a per-segment level using the 18-segment model of the Society of Cardiovascular Computed Tomography [26]. For analysis, the mean of both observers was calculated. To analyse the image quality on a per-patient level, the mean image quality on a per-vessel level was calculated as previously described [13]. To obtain the per-vessel image quality score, the highest score of any coronary artery segment of the corresponding coronary artery was chosen. Not all 18 coronary artery segments were present in every patient. A total of 292 coronary segments were available for analysis. In one patient, there were separate ostia of the left anterior descending and the left

circumflex coronary artery, so that a left main artery was missing.

Attenuation, image noise, signal-to-noise and contrast-to-noise ratio

To evaluate objective parameters of image quality, the image noise, signal-to-noise ratio (SNR) and contrast-to-noise ratio (CNR) were measured. Image noise was determined by measuring the standard deviation (SD) of CT attenuation values in a circular region of interest (mean 4.5±1.3 cm^2) placed in the ascending aorta at the level of the left main coronary artery (see Fig. 1). The signal-to-noise ratio (SNR) and contrast-to-noise ratio (CNR) were obtained in the proximal coronary arteries as previously described [13, 27]. In brief, attenuation of the coronary arteries was measured by placing a region of interest in the lumen of the coronary artery. The region of interest was chosen as large as possible without including parts of the vessel wall. To obtain the CT attenuation in the surrounding tissue, a region of interest was placed next to the vessel wall. SNR was calculated as the quotient of mean attenuation of the coronary artery and image noise. CNR was determined by dividing contrast attenuation by image noise.

Effective radiation dose

The effective radiation dose was derived from the dose length product (DLP) and a conversion factor of 0.014 for chest CT in adults according to Bongartz et al. [28, 29].

Statistical analysis

Statistical analyses were performed using Microsoft Excel (2010) and Graph Pad Prism Version 5.01 (Graph Pad Software, San Diego, CA, USA). Continuous variables are expressed as mean ± SD and categoric variables are expressed as frequencies or percentages. To compare the image quality of FBP and SAFIRE reconstruction algorithms, a Mann-Whitney *U*-test was used for continuous variables and a Fisher's exact test was used for categoric variables. For paired observations, a Wilcoxon matched pairs test was used for continuous variables. *P* values<0.05 were considered to be statistically significant. Weighted Cohen's kappa coefficients (κ-values) were calculated for the assessment of interobserver agreements of image quality on a per-vessel level. κ-Values were interpreted as follows: absence of agreement ≤0, poor agreement <0.20, fair agreement 0.21–0.40, moderate agreement 0.41–0.60, good agreement 0.61–0.80 and excellent agreement >0.80.

Results

Characteristics of the study population are shown in Table 1. The mean age of all 21 individuals (13 males) was 52± 14 years. The mean body weight was 71.5±12.2 kg and mean height was 173±7 cm with a corresponding body mass index (BMI) of 23.9±3.2 kg/m^2. Mean heart rate during coronary CT angiography was 50±6 beats per minute (bpm) (range 40 to 60 bpm). Mean dose length product was 4.6±0.5 mGy*cm, which corresponds to an average effective dose of 0.06±0.01 mSv (range 0.06 to 0.07 mSv).

Image quality

In images reconstructed with filtered back projection, the mean image quality score per segment was 2.2±1.0, whereas the mean image quality score was 1.9±1.1 in images with the SAFIRE reconstruction algorithm, indicating a higher image quality with the SAFIRE reconstruction algorithm (*P* <0.0001). On a per-patient analysis, mean image quality was 2.4±1.1 for FBP and 2.1±1.1 for iterative reconstruction (*P*<0.0001, see Fig. 2).

Of 292 coronary segments, 55 (18.8 %) were unevaluable in FBP and 40 (13.7 %) were unevaluable in IR (p=0.12). In FBP, 59 of 83 (71.1 %) vessels and 12 of 21 individuals (57.1 %) were fully evaluable (no unevaluable segment). In

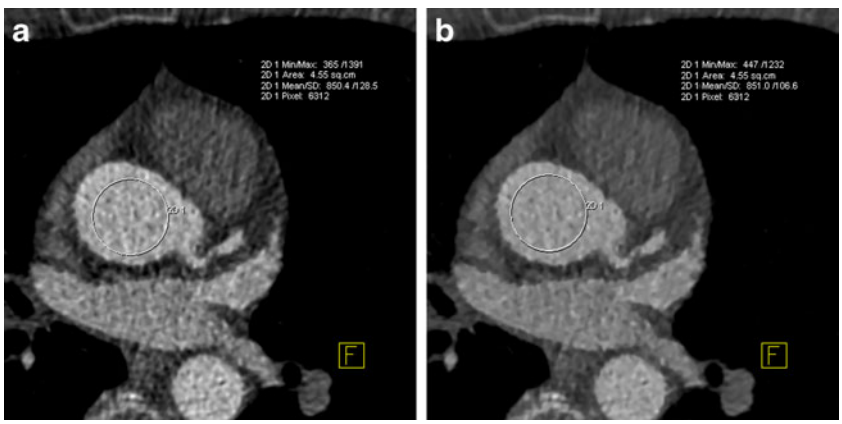

Fig. 1 Measurement of image noise in the aorta at the level of the left main coronary artery in a 52-year-old male patient (62 kg, 178 cm). **a** Measurement of image noise in filtered back projection (region of interest shows image noise is 128.5 HU). **b** Measurement of image noise in iterative reconstruction (region of interest shows image noise is 106.6 HU)

Table 1 Characteristics of the study cohort

Characteristic	Values
Age (years)	52±14
Gender (male)	13/21 (61.9 %)
Body weight (kg)	71.5±12.2
Body height (m)	1.73±0.07
BMI (kg/m^2)	23.9±3.2
Heart rate (beats per minute)	50±6
Dose length product (mGy*cm)	4.6±0.5
Effective dose (mSv)	0.06±0.01

IR, 66 of 83 (79.5 %, p=0.28) vessels and 12 of 21 individuals (57.1 %) were fully evaluable (no unevaluable segment).

In FBP, for individuals with a body weight ≤75 kg (n=12) as compared to a body weight >75 kg (n=9), the rates of fully evaluable segments [156/163 (95.7 %) vs. 81/129 (62.8 %); P<0.0001] and vessels [44/47 (93.6 %) vs. 15/36 (41.7 %); P<0.0001, see Table 2] were significantly higher (see Fig. 3). The majority of individuals with a body weight ≤75 kg [10/12 (83.3 %)] were fully evaluable (no unevaluable segment), whereas a minority of individuals with a body weight >75 kg [2/9 (22.2 %), P=0.003] were fully evaluable.

In IR, for individuals with a body weight ≤75 kg (n=12) as compared to a body weight >75 kg (n=9), the rates of fully evaluable segments [159/163 (97.5 %) vs. 93/129 (72.1 %); P<0.0001] and vessels [45/47 (95.7 %) vs. 21/36 (58.3 %), P<0.0001, see Table 2] were significantly higher. Ten of 12 individuals with a body weight ≤75 kg (83.3 %) were fully evaluable (no unevaluable segment), whereas only 2 of 9 patients with a body weight >75 kg (22.2 %, P=0.003) were fully evaluable.

Attenuation, image noise, signal-to-noise and contrast-to-noise ratio

Mean attenuation in the aorta at the level of the left main coronary artery was 721.9±133.3 HU in FBP and 711.9±134.7 HU in the SAFIRE reconstruction algorithm (P=0.88).

Mean image noise was 158.2±44.7 HU in FBP and 128.9±46.6 HU in the SAFIRE reconstruction algorithm, showing a significant reduction of image noise in images reconstructed with the iterative reconstruction algorithm (P=0.02).

In the whole study cohort, there were no significant differences in signal, contrast, signal-to-noise or contrast-to-noise ratios in the coronary arteries between images reconstructed in FBP and the SAFIRE reconstruction algorithm (see Table 3). In FBP, individuals with a body weight ≤75 kg showed significantly higher signals, contrast, signal-to-noise and contrast-to-noise ratios in all coronary arteries in comparison to individuals with a body weight >75 kg (see Table 4), except for the signal of the right coronary artery (P=0.06). In SAFIRE, in individuals with a body weight ≤75 kg compared to patients with a body weight >75 kg, there were also significantly higher signals, contrasts, signal-to-noise and contrast-to-noise ratios (see Table 4).

Individuals with a body weight ≤75 kg showed significantly lower image noise in images reconstructed using SAFIRE as compared to FBP. There were no significant differences in signal and contrast of the coronary arteries in FBP and in SAFIRE. However, as image noise was lower, signal-to-noise and contrast-to-noise ratios showed significantly higher results in the iterative reconstruction algorithm in comparison to filtered back projection. However, there were no significant differences between FBP and the iterative reconstruction algorithm in individuals with a body weight >75 kg (see Table 5).

Interobserver variability

On a per-vessel level, interobserver agreement concerning the subjective image quality score was moderate for images reconstructed by filtered back projection (2.2±1.3 vs. 2.5±1.1, κ=0.57) and also moderate for the iterative reconstruction algorithm (1.9±1.3 vs. 2.3±1.1, κ=0.53).

In individuals with a body weight ≤75 kg, there was a significant difference in the subjective image quality score between both observers in FBP (1.4±0.9 vs. 2.1±1.4, P<0.0001) as well as in the SAFIRE reconstruction algorithm (1.3±0.8 vs. 1.9±1.1, P<0.0001). Interobserver agreement was only fair for both reconstruction algorithms (κ=0.34 or 0.30, respectively).

In individuals with a body weight >75 kg, the subjective image quality score did not differ significantly between the two observers for FBP (3.3±0.9 vs. 3.1±0.9, P=0.06) and the SAFIRE reconstruction algorithm (2.8±1.3 vs 2.9±1.0; P=0.5). Interobserver agreement was good for FBP (κ=0.61) and moderate for the SAFIRE reconstruction algorithm (κ=0.56).

Discussion

In the last years, substantial efforts have been undertaken to reduce radiation exposure in coronary CT angiography. Besides technical advances in CT hardware and acquisition protocols, the computational power now allows more elaborate reconstruction algorithms that reduce image noise and improve image quality. Preliminary studies have shown that these so-called “iterative reconstruction algorithms” have the potential to reduce radiation dose exposure in chest [22], abdominal [23], body [17], and cardiac CT [18, 20, 21, 24, 25, 30].

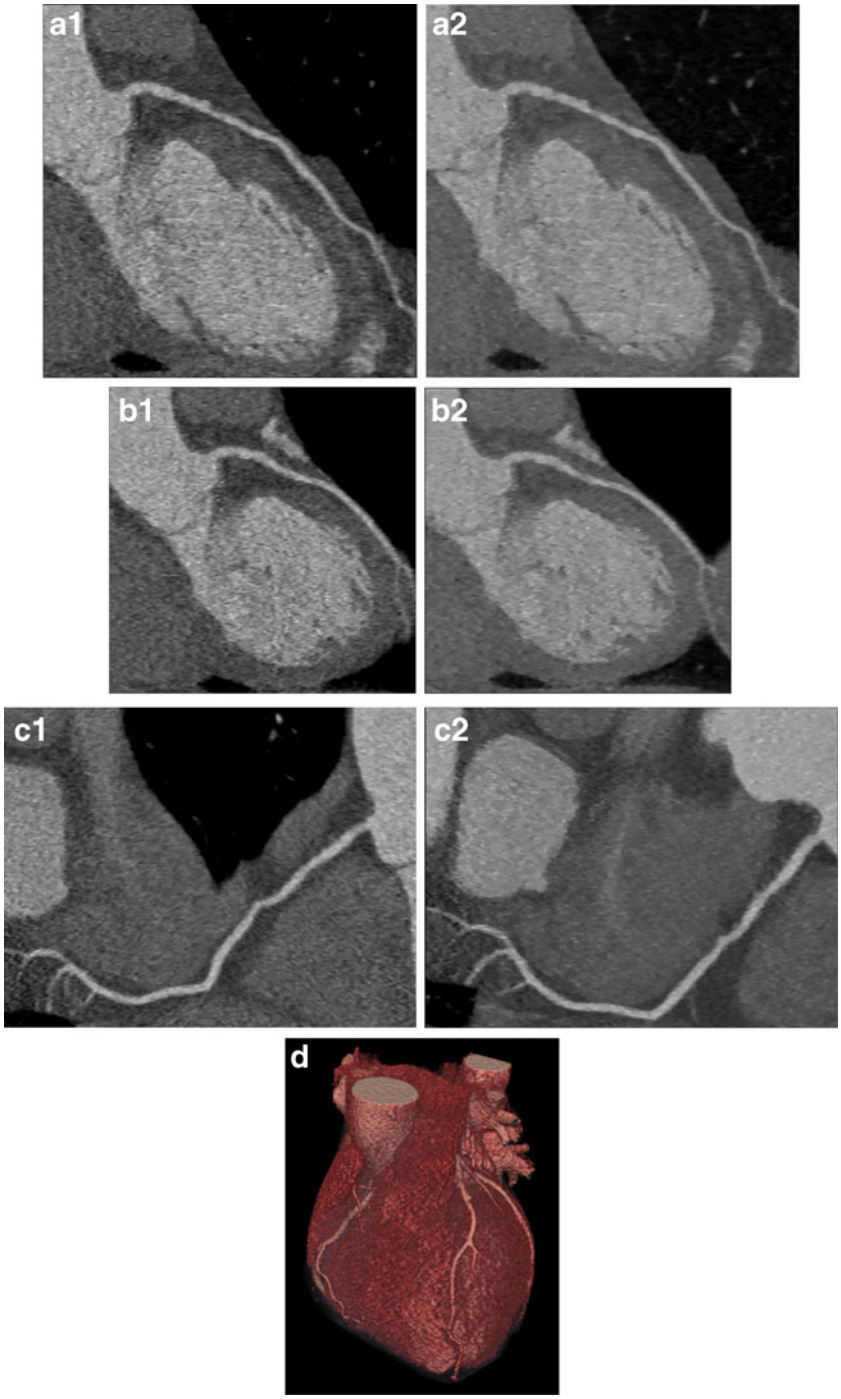

Fig. 2 Coronary CT angiography images of a 52-year-old male patient (62 kg, 178 cm, heart rate 60 beats per minute) obtained by prospectively ECG-triggered high-pitch spiral acquisition (80-kV tube voltage, 50-mAs tube current, DLP 5 mGy*cm estimated effective dose 0.07 mSv) reconstructed by iterative reconstruction algorithm: No coronary artery stenoses are present. **a** Curved multiplanar reconstruction of the left anterior descending coronary artery in FBP (*A1*) and SAFIRE reconstruction algorithm (*A2*). **b** Curved multiplanar reconstruction of the left circumflex coronary artery in FBP (*B1*) and SAFIRE reconstruction algorithm (*B2*). **c** Curved multiplanar reconstruction of the right coronary artery in FBP (*C1*) and SAFIRE reconstruction algorithm (*C2*). **d** Three-dimensional, surface-weighted reconstruction of the heart and coronary arteries

Table 2 Subjective image quality parameters: number of fully evaluable coronary segments, vessels and patients

	FBP			SAFIRE		
	≤75 kg (*n*=12)	>75 kg (*n*=9)	*P*-value	≤75 kg (*n*=12)	>75 kg (*n*=9)	*P*-value
Coronary segments	156/163 (95.7 %)	81/129 (62.8 %)	<0.0001	159/163 (97.5 %)	93/129 (72.1 %)	<0.0001
Coronary vessels	44/47 (93.6 %)	15/36 (41.7 %)	<0.0001	45/47 (95.7 %)	21/36 (58.3 %)	<0.0001
Per patient	10/12 (83.3 %)	2/9 (22.2 %)	0.0003	10/12 (83.3 %)	2/9 (22.2 %)	0.0003

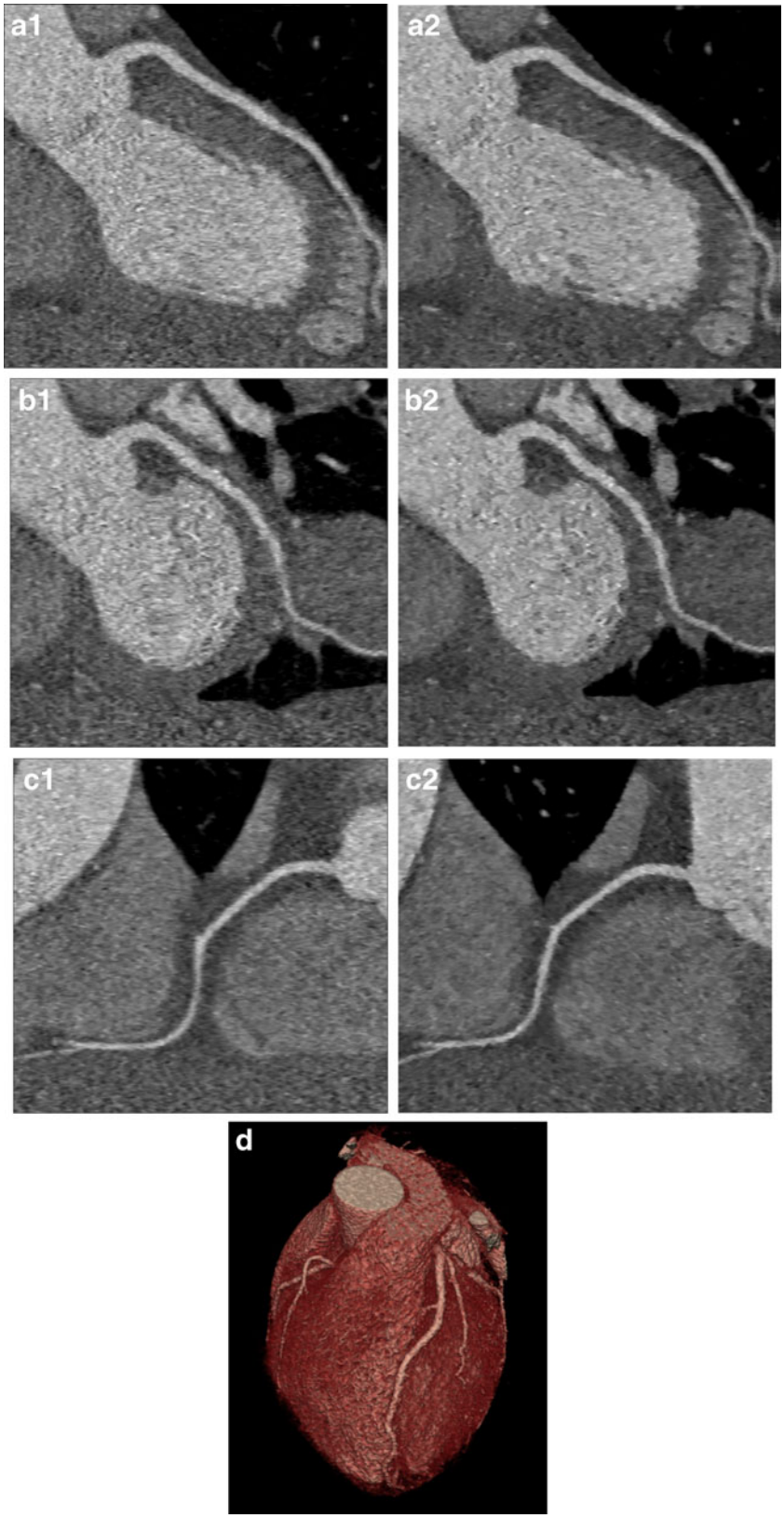

Fig. 3 Coronary CT angiography images of a 49-year-old male patient (62 kg, 170 cm, heart rate 53 beats per minute) obtained by prospectively ECG-triggered high-pitch spiral acquisition (80 kV tube voltage, 50 mAs tube current, DLP 4 mGy*cm estimated effective dose 0.06 mSv) reconstructed by iterative reconstruction algorithm: No coronary artery stenoses are present. All segments were graded as "evaluable" by both observers. **a** Curved multiplanar reconstruction of the left anterior descending coronary artery in FBP (*A1*) and SAFIRE reconstruction algorithm (*A2*). **b** Curved multiplanar reconstruction of the left circumflex coronary artery in FBP (*B1*) and SAFIRE reconstruction algorithm (*B2*). **c** Curved multiplanar reconstruction of the right coronary artery in FBP (*C1*) and SAFIRE reconstruction algorithm (*C2*). **d** Three-dimensional, surface weighted reconstruction of the heart and coronary arteries

In our study, the iterative reconstruction algorithm led to a significant reduction in image noise (158.2±44.7 in FBP vs. 128.9±46.6 in SAFIRE, $P=0.02$) and to a significant improvement in subjective image quality (2.2±1.0 in FBP vs. 1.9±1.1 in SAFIRE, $P<0.0001$) in the overall study cohort. This is in agreement with previous studies [18–21,

Table 3 Objective image quality parameters of the overall study cohort

	Filtered back projection (FBP)	Iterative reconstruction (SAFIRE)	Significance *P*-value
Aorta signal (HU)	721.9±133.3	711.9±134.7	n.s. (0.88)
Aorta noise (HU)	158.2±44.7	128.9±46.6	0.02
LM signal (HU)	734.8±163.6	710.6±148.0	n.s. (0.80)
LM contrast (HU)	773.9±182.1	728.3±138.3	n.s. (0.48)
LM SNR	5.0±1.8	6.3±2.7	n.s. (0.15)
LM CNR	5.2±1.8	6.4±2.4	n.s. (0.11)
LAD signal (HU)	733.4±129.4	698.6±183.9	n.s. (0.47)
LAD contrast (HU)	773.7±141.2	728.5±179.8	n.s. (0.42)
LAD SNR	5.0±1.5	6.2±2.8	n.s. (0.14)
LAD CNR	5.3±1.6	6.4±2.7	n.s. (0.13)
LCX signal (HU)	724.8±182.4	710.8±175.7	n.s. (0.76)
LCX contrast (HU)	763.1±185.9	726.8±190.5	n.s. (0.99)
LCX SNR	5.1±1.8	6.4±2.8	n.s. (0.11)
LCX CNR	5.3±1.8	6.6±3.1	n.s. (0.10)
RCA signal (HU)	769.3±173.9	758.6±190.8	n.s. (0.76)
RCA contrast (HU)	853.6±166.6	797.7±184.1	n.s. (0.37)
RCA SNR	5.2±1.8	6.6±2.7	n.s. (0.11)
RCA CNR	5.7±1.9	7.0±2.8	n.s. (0.18)

SNR signal-to-noise ratio, *CNR* contrast-to-noise ratio, *LM* left main coronary artery, *LAD* left anterior descending coronary artery, *LCX* left circumflex coronary artery, *RCA* right coronary artery

Table 4 Objective image quality parameters: comparison between individuals with a body weight ≤75 kg and >75 kg

	Filtered back projection (FBP)			Iterative reconstruction (SAFIRE)		
	≤75 kg	>75 kg	*P*-value	≤75 kg	>75 kg	*P*-value
Aorta signal (HU)	804.1±95.1	612.4±91.4	0.0009	790.1±103.3	607.7±96.6	0.001
Aorta noise (HU)	139.9±26.9	182.6±53.2	0.03	109.5±35.1	154.8±49.1	0.02
LM signal (HU)	829.2±160.4	619.5±64.5	0.004	795.4±111.9	597.7±111.4	0.002
LM contrast (HU)	865.3±179.0	662.1±114.5	0.02	792.1±97.5	643.4±143.4	0.03
LM SNR	6.1±1.5	3.7±1.1	0.0008	7.8±2.3	4.2±1.4	0.002
LM CNR	6.3±1.4	3.9±1.1	0.001	7.8±2.1	4.5±1.4	0.002
LAD signal (HU)	806.5±110.5	636.0±80.1	0.002	804.0±143.8	558.1±131.3	0.002
LAD contrast (HU)	846.5±135.7	676.6±77.5	0.01	828.2±139.5	595.5±138.7	0.002
LAD SNR	5.9±1.1	3.8±1.1	0.001	7.9±2.4	4.0±1.7	0.002
LAD CNR	6.2±1.3	4.0±1.1	0.0009	8.1±2.1	4.3±1.8	0.002
LCX signal (HU)	822.9±141.8	577.5±132.0	0.001	803.9±138.4	571.1±128.4	0.002
LCX contrast (HU)	870.6±138.8	602.0±118.5	0.001	831.4±114.3	569.9±176.1	0.0006
LCX SNR	6.1±1.4	3.6±1.3	0.004	7.9±2.3	4.1±2.0	0.002
LCX CNR	6.4±1.2	3.7±1.3	0.002	8.2±2.3	4.2±2.4	0.004
RCA signal (HU)	841.1±124.6	681.6±191.6	n.s. (0.06)	859.1±147.1	624.6±161.0	0.006
RCA contrast (HU)	921.1±129.6	771.2±176.1	0.05	893.7±148.6	669.7±148.8	0.005
RCA SNR	6.2±1.5	4.0±1.5	0.006	8.3±2.1	4.4±1.6	0.0007
RCA CNR	6.7±1.5	4.5±1.6	0.01	8.7±2.1	4.7±1.6	0.0007

SNR signal-to-noise ratio, *CNR* contrast-to-noise ratio, *LM* left main coronary artery, *LAD* left anterior descending coronary artery, *LCX* left circumflex coronary artery, *RCA* right coronary artery

Table 5 Objective image quality parameters: comparison between FBP and SAFIRE reconstruction algorithm in individuals with a body weight ≤75 kg and >75 kg

	≤75 kg			>75 kg		
	FBP	SAFIRE	*P*-value	FBP	SAFIRE	*P*-value
Aorta signal (HU)	804.1±95.1	790.1±103.3	n.s. (0.79)	612.4±91.4	607.7±96.6	n.s. (0.80)
Aorta noise (HU)	139.9±26.9	109.5±35.1	0.01	182.6±53.2	154.8±49.1	n.s. (0.30)
LM signal (HU)	829.2±160.4	795.4±111.9	n.s. (0.73)	619.5±64.5	597.7±111.4	n.s. (0.34)
LM contrast (HU)	865.3±179.0	792.1±97.5	n.s. (0.36)	662.1±114.5	643.4±143.4	n.s. (0.49)
LM SNR	6.1±1.5	7.8±2.3	0.04	3.7±1.1	4.2±1.4	n.s. (0.54)
LM CNR	6.3±1.4	7.8±2.1	0.03	3.9±1.1	4.5±1.4	n.s. (0.39)
LAD signal (HU)	806.5±110.5	804.0±143.8	n.s. (0.98)	636.0±80.1	558.1±131.3	n.s. (0.09)
LAD contrast (HU)	846.5±135.7	828.2±139.5	n.s. (0.71)	676.6±77.5	595.5±138.7	n.s. (0.16)
LAD SNR	5.9±1.1	7.9±2.4	0.01	3.8±1.1	4.0±1.7	n.s. (1.0)
LAD CNR	6.2±1.3	8.1±2.1	0.02	4.0±1.1	4.3±1.8	n.s. (0.93)
LCX signal (HU)	822.9±141.8	803.9±138.4	n.s. (0.79)	577.5±132.0	571.1±128.4	n.s. (0.88)
LCX contrast (HU)	870.6±138.8	831.4±114.3	n.s. (0.47)	602.0±118.5	569.9±176.1	n.s. (0.72)
LCX SNR	6.1±1.4	7.9±2.3	0.02	3.6±1.3	4.1±2.0	n.s. (0.72)
LCX CNR	6.4±1.2	8.2±2.3	0.02	3.7±1.3	4.2±2.4	n.s. (0.72)
RCA signal (HU)	841.1±124.6	859.1±147.1	n.s. (0.83)	681.6±191.6	624.6±161.0	n.s. (0.49)
RCA contrast (HU)	921.1±129.6	893.7±148.6	n.s. (0.83)	771.2±176.1	669.7±148.8	n.s. (0.26)
RCA SNR	6.2±1.5	8.3±2.1	0.02	4.0±1.5	4.4±1.6	n.s. (0.80)
RCA CNR	6.7±1.5	8.7±2.1	0.03	4.5±1.6	4.7±1.6	n.s. (0.86)

SNR signal-to-noise ratio, *CNR* contrast-to-noise ratio, *LM* left main coronary artery, *LAD* left anterior descending coronary artery, *LCX* left circumflex coronary artery, *RCA* right coronary artery

25]. However, to our knowledge, there is no study that combined the prospectively ECG-triggered high-pitch spiral acquisition mode with low-voltage and low-current acquisition as well as iterative reconstruction. While the study of Utsunomiya et al. on the effect of the iterative reconstruction technique on image quality was performed using a prospectively gated 256-slice CT [21], Leipsic et al. used prospective and retrospective gating in their studies on iterative reconstruction algorithms in cardiac CT [19, 24]. Bittencourt et al. showed that using the prospectively ECG-triggered high-pitch spiral acquisition mode in conjunction with an iterative reconstruction algorithm led to a reduction in image noise of 26±10 % [18], which is comparable to our study with an image noise reduction of 24 %±11 %. Like data of other groups, our data of the whole study cohort show that mean contrast attenuation and contrast enhancement in the aorta and in the proximal coronary arteries do not differ between both reconstruction algorithms [18–21]. Signal-to-noise and contrast-to-noise ratios were not significantly different for the whole study cohort and in the subgroup of patients with a body weight >75 kg. However, in the subgroup of patients with a body weight ≤75 kg, signal-to-noise and contrast-to-noise ratios were significantly higher for images reconstructed by the iterative reconstruction algorithm, which may be due to the reduced image noise. This is also in agreement with previous studies [18, 19, 21].

While interobserver agreement concerning the image quality score was excellent for iterative and FBP reconstruction algorithms (κ=0.89 and 0.84, respectively) in the study by Moscariello et al. [20], in our study, interobserver agreement for image quality was only moderate for both reconstruction algorithms (κ=0.53 and 0.57, respectively). In subgroup analysis, interobserver agreement was good for FBP (κ=0.61) and moderate (κ=0.56) for iterative reconstruction in patients with body weight>75 kg. One reason for an only fair interobserver agreement in patients with a body weight ≤75 kg (κ=0.34 in FBP and κ=0.30 in SAFIRE) might be the fact that image quality scores were significantly different for both observers (in FBP: 1.4±0.9 vs. 2.1±1.4, P<0.0001, and 1.3±0.8 vs. 1.9±1.1, P<0.0001 in SAFIRE).

Although our study demonstrates the ability to perform coronary CT angiography with an ultra-low radiation exposure of <0.1 mSv in a selected cohort of individuals with a low and stable heart rate of ≤60 beats per minute as well as a body weight <100 kg, there are several limitations to consider. First of all, in this feasibility study, entry criteria were strict and the study cohort was small. Larger studies will be necessary to confirm our findings in a clinical context.

Secondly, only few individuals presented with coronary atherosclerotic plaque, and results might be worse in patients with a high coronary plaque burden. While we thoroughly analysed image quality, accuracy for stenosis detection was not determined, and the sample size would have been too small to do that. Measuring image noise by determining the standard deviation of attenuation values in a region of interest assumed to be of homogenous density is an imperfect marker of image quality and does not necessarily allow a conclusion about the image quality in two different reconstructions. While we were able to report on the image quality of coronary CT angiography performed at very low dose, no gold standard for comparison was available. No statement concerning diagnostic accuracy can therefore be made. Further studies are needed to validate the diagnostic accuracy of ultra-low radiation acquisition protocols, for example, in comparison to invasive coronary angiography, the standard of reference. Finally, we did not randomise the individuals to other acquisition modes. To achieve this ultra-low radiation exposure, we used the prospectively ECG-triggered high-pitch spiral acquisition mode, which can be vulnerable to artefacts, e.g. to motion artefacts if the heart rate is not low and very stable [31]. As our data show, in individuals with a body weight of >75 kg, diagnostic image quality is limited, and hence, we would currently not recommend the use of this ultra-low radiation acquisition protocol in patients with a body weight >75 kg, as the number of not fully interpretable examinations may be too high. Hence, the overall number of patients who would be candidates for this acquisition protocol is limited. However, ultra-low dose CT might be an option in patients of young age and low to intermediate risk for coronary artery disease, and in individuals who need to undergo coronary CT angiography for reasons other than stenosis detection, e.g. the analysis of coronary anomalies, or non-coronary cardiac CT.

In conclusion, this preliminary study shows that the combination of prospectively ECG-triggered high-pitch spiral acquisition, tube voltage of 80 kV and tube current of 50 mAs with raw data-based iterative reconstruction algorithm allows coronary CT angiography with ultra-low radiation exposure of <0.1 mSv in patients with a body weight ≤75 kg and a stable heart rate ≤60 beats per minute.

Acknowledgments This study was supported by the German Government, Bundesministerium für Bildung und Forschung (01EX1012B, "Spitzencluster Medical Valley")

References

1. Achenbach S, Goroll T, Seltmann M et al (2011) Detection of coronary artery stenoses by low dose, prospectively ECG-triggered, high-pitch spiral coronary CT angiography. JACC Cardiovasc Imaging 4:328–337
2. Budoff MJ, Dowe D, Jollis JG et al (2008) Diagnostic performance of 64-multidetector row coronary computed tomographic angiography for evaluation of coronary artery stenosis in individuals without known coronary artery disease: results from the prospective multicenter ACCURACY (Assessment by Coronary Computed Tomographic Angiography of Individuals Undergoing Invasive Coronary Angiography) trial. J Am Coll Cardiol 52:1724–1732
3. Chow BJ, Wells GA, Chen L et al (2010) Prognostic value of 64-slice cardiac computed tomography severity of coronary artery disease, coronary atherosclerosis, and left ventricular ejection fraction. J Am Coll Cardiol 55:1017–1028
4. Kerl JM, Schoepf UJ, Zwerner PL et al (2011) Accuracy of coronary artery stenosis detection with CT versus conventional coronary angiography compared with composite findings from both tests as an enhanced reference standard. Eur Radiol 21:1895–1903
5. van Velzen JE, Schuijf JD, de Graaf FR et al (2011) Diagnostic performance of non-invasive multidetector computed tomography coronary angiography to detect coronary artery disease using different endpoints: detection of significant stenosis vs. detection of atherosclerosis. Eur Heart J 32:637–645
6. Hausleiter J, Meyer T, Hermann F et al (2009) Estimated radiation dose associated with cardiac CT angiography. JAMA 30:500–507
7. Einstein AJ, Elliston CD, Arai AE et al (2010) Radiation dose from single-heartbeat coronary CT angiography performed with a 320-detector row volume scanner. Radiology 254:698–706
8. Stolzmann P, Leschka S, Scheffel H et al (2008) Dual-source CT in step-and-shoot mode: noninvasive coronary angiography with low radiation dose. Radiology 249:71–80
9. Scheffel H, Alkadhi H, Leschka S et al (2008) Low-dose CT coronary angiography in the step-and-shoot mode: diagnostic performance. Heart 94:1132–1137
10. Achenbach S, Marwan M, Schepis T et al (2009) High-pitch spiral acquisition: a new scan mode for coronary CT angiography. J Cardiovasc Comput Tomogr 3:117–121
11. Achenbach S, Marwan M, Ropers D et al (2010) Coronary computed tomography angiography with a consistent dose below 1 mSv using prospectively electrocardiogram-triggered high-pitch spiral acquisition. Eur Heart J 31:340–346
12. Vorobiof G, Achenbach S, Narula J (2012) Minimizing radiation dose for coronary CT angiography. Cardiol Clin 30:9–17
13. Pflederer T, Rudofsky L, Ropers D et al (2009) Image quality in a low radiation exposure protocol for retrospectively ECG-gated coronary CT angiography. AJR Am J Roentgenol 192:1045–1050
14. Bischoff B, Hein F, Meyer T et al (2009) Impact of a reduced tube voltage on CT angiography and radiation dose: results of the PROTECTION I study. JACC Cardiovasc Imaging 2:940–946
15. Leschka S, Stolzmann P, Schmid FT et al (2008) Low kilovoltage cardiac dual-source CT: attenuation, noise, and radiation dose. Eur Radiol 18:1809–1817
16. Blankstein R, Bolen MA, Pale R et al (2011) Use of 100 kV versus 120 kV in cardiac dual source computed tomography: effect on radiation dose and image quality. Int J Cardiovasc Imaging 27:579–586
17. Winklehner A, Karlo C, Puippe G et al (2011) Raw data-based iterative reconstruction in body CTA: evaluation of radiation dose saving potential. Eur Radiol 21:2521–2526
18. Bittencourt MS, Schmidt B, Seltmann M et al (2011) Iterative reconstruction in image space (IRIS) in cardiac computed tomography: initial experience. Int J Cardiovasc Imaging 27:1081–1087
19. Leipsic J, LaBounty TM, Heilbron G et al (2010) Adaptive statistical iterative reconstruction: assessment of image noise and image quality in coronary CT angiography. AJR Am J Roentgenol 195:649–654

20. Moscariello A, Takx RA, Schoepf UJ et al (2011) Coronary CT angiography: image quality, diagnostic accuracy, and potential for radiation dose reduction using a novel iterative image reconstruction technique-comparison with traditional filtered back projection. Eur Radiol 21:2130–2138
21. Utsunomiya D, Weigold WG, Weissman G et al (2012) Effect of hybrid iterative reconstruction technique on quantitative and qualitative image analysis at 256-slice prospective gating cardiac CT. Eur Radiol 22:1287–1294
22. Leipsic J, Nguyen G, Brown J et al (2010) A prospective evaluation of dose reduction and image quality in chest CT using adaptive statistical iterative reconstruction. AJR Am J Roentgenol 195:1095–1099
23. Marin D, Nelson RC, Schindera ST et al (2010) Low-tube-voltage, high-tube-current multidetector abdominal CT: improved image quality and decreased radiation dose with adaptive statistical iterative reconstruction algorithm–initial clinical experience. Radiology 254:145–153
24. Leipsic J, Labounty TM, Heilbron B et al (2010) Estimated radiation dose reduction using adaptive statistical iterative reconstruction in coronary CT angiography: the ERASIR study. AJR Am J Roentgenol 195:655–660
25. Renker M, Ramachandra A, Schoepf UJ et al (2011) Iterative image reconstruction techniques: applications for cardiac CT. J Cardiovasc Comput Tomogr 5:225–230
26. Raff GL, Abidov A, Achenbach S et al (2009) SCCT guidelines for the interpretation and reporting of coronary computed tomographic angiography. J Cardiovasc Comput Tomogr 3:122–136
27. Achenbach S, Giesler T, Ropers D et al (2006) Comparison of image quality in contrast-enhanced coronary artery visualization by electron-beam tomography and retrospectively electrocardiogram-gated multislice spiral computed tomography. Eur J Radiol 57:373–379
28. Bongartz G, Golding SJ, Jurik AG et al (2004) European Guidelines for Multislice Computed Tomography: Appendix C Funded by the European Commission. Contract number FIGM-CT2000-20078-CT-TIP. Available via http://w3.tue.nl/fileadmin/sbd/Documenten/`Leergang/BSM/European_Guidelines_Quality_Criteria_Computed_Tomography_Eur_16252.pdf. Accessed 04 June 2012
29. Halliburton SS, Abbara S, Chen MY et al (2011) SCCT guidelines on radiation dose and dose-optimization strategies in cardiovascular CT. J Cardiovasc Comput Tomogr 5:198–224
30. Gosling O, Loader R, Venables P et al (2010) A comparison of radiation doses between state-of-the-art multislice CT coronary angiography with iterative reconstruction, multislice CT coronary angiography with standard filtered back-projection and invasive diagnostic coronary angiography. Heart 96:922–926
31. Neefjes LA, Dharampal AS, Rossi A et al (2011) Image quality and radiation exposure using different low-dose scan protocols in dual-source CT coronary angiography: randomized study. Radiology 261:779–786